20 p.

NASA TECHNICAL NOTE

NASA TN D-1876

NASA TN D-1876

STUDY OF THE EFFECT OF A CLOSED-END SIDE BRANCH ON SINUSOIDALLY PERTURBED FLOW OF LIQUID IN A LINE

by William Lewis, Robert J. Blade, and Robert G. Dorsch;
Lewis Research Center,
Cleveland, Ohio

NATIONAL AERONAUTICS AND SPACE ADMINISTRATION • WASHINGTON, D. C. • SEPTEMBER 1963

TECHNICAL NOTE D-1876

STUDY OF THE EFFECT OF A CLOSED-END SIDE BRANCH ON SINUSOIDALLY PERTURBED FLOW OF LIQUID IN A LINE

By William Lewis, Robert J. Blade,
and Robert G. Dorsch

Lewis Research Center
Cleveland, Ohio

NATIONAL AERONAUTICS AND SPACE ADMINISTRATION

NATIONAL AERONAUTICS AND SPACE ADMINISTRATION

TECHNICAL NOTE D-1876

STUDY OF THE EFFECT OF A CLOSED-END SIDE BRANCH ON SINUSOIDALLY PERTURBED FLOW OF LIQUID IN A LINE

By William Lewis, Robert J. Blade,
and Robert G. Dorsch

SUMMARY

Classical undamped acoustic-wave theory was used to determine analytical relations among sinusoidal perturbations of pressure and flow at the ends of a hydraulic-transmission line having a closed-end branch of arbitrary length attached at an arbitrary point. Experimental data were obtained for the equilateral case (a branch half as long as the main line connected to the main line at the midpoint) at mean flow speeds of 5 to 10 feet per second. Measured pressure-perturbation ratios agreed closely with analytical predictions. At frequencies for which the branch length was an odd multiple of 1/4 wavelength, waves in the main line were almost completely reflected at the junction point.

INTRODUCTION

Acoustic pressure and flow perturbations in long hydraulic lines are often of importance in the operation of various fluid systems. Among these are hydraulic control systems (ref. 1) and rocket propellant systems (ref. 2). Because of the need to predict acoustic effects in fluid systems for rocket and space applications, the NASA Lewis Research Center has undertaken a study of acoustic disturbances in flowing-liquid systems. An investigation of acoustic waves in a long straight line rigidly supported at one end is reported in reference 3. The effect of longitudinal pipe motion produced by unbalanced pressure forces on an elbow is treated in reference 4.

This report presents the results of a study concerning the effects of a closed branch on acoustic disturbances in a line. A general analysis based on classical acoustic-wave theory is presented. This analysis shows the effect of a closed branch of arbitrary length attached to the main line at an arbitrary point when the line is terminated in an arbitrary impedance. Experimental results are given for a particular configuration in which a 34-foot closed branch was attached at the midpoint of a line 68 feet long that terminated in a resistive impedance. The main line and branch were of stainless-steel tube 1.00 inch in outside diameter with a 0.065-inch wall. The experiment covered a range of disturbance frequencies from 0.5 to 82.0 cycles per second, mean flow speed in the main line from 5 to 10 feet per second, and mean line pressure from 50 to 225 pounds per square inch gage. The average amplitude of the sinusoidal perturbation was about 5 pounds per square inch for pressure and 0.13 foot per second

for fluid velocity. The flow of the fluid (JP-4 fuel) was modulated by means of a hydraulic servovalve at the upstream end and was restricted by an orifice at the downstream end.

EXPERIMENTAL SYSTEM

Apparatus

Flow system. - The essential parts of the open-loop pumped-return flow system used in the experiment are shown in figure 1. The fluid (JP-4 fuel) was forced through the test line by a gear pump, and the mean flow rate was measured by the use of a rotameter. Hydraulic accumulators were placed between the pump and the test line to provide steady supply pressure. The discharge from the test line was submerged in a constant-height vented tank. Fluid was returned to the supply tank by intermittent operation of the return pump.

Flow disturbance generator. - Sinusoidal perturbations of flow and pressure were induced in the system by means of an electrohydraulic throttle servovalve located just upstream of the test line. The throttle was oscillated sinusoidally about a partly open mean position in response to an alternating voltage. A porous-metal filter was placed between the throttle and the test line to reduce turbulence.

Test line. - The test line, made of stainless-steel tubing having a 1.000-inch outside diameter and a 0.065-inch wall thickness, was fitted with a right-angle tee at the midpoint. Attached to the tee was a 34-foot branch line of the same tubing that was closed at the end by a rigid cap. Provision was made for bleeding the line to get rid of air. The closed end of the branch and both ends of the main line were clamped to rigid supports in order to avoid pipe-motion effects of the type described in reference 4. The downstream end was terminated in an orifice plate containing 34 holes 0.040 inch in diameter.

Instrumentation. - Instrument sensing elements to measure pressure perturbations were located at stations A, B, C, D, E, and F, as shown in figure 1. The pressure sensors were commercial flush-diaphram units. Pressure perturbations in pounds per square foot were obtained by means of static calibration of each unit with its associated amplifier. The in-phase and quadrature components of the pressure perturbations were read from a commercial transfer-function analyzer, as in the investigations previously reported (refs. 3 and 4).

Procedure

The flow system was operated at constant mean flow rate and pressure until conditions had stabilized. The branch line was bled at the closed end to ensure that no air was trapped in the system. Mean flow rate and pressures at stations A and E were recorded. The throttle was operated at frequencies of 0.5 to 82.0 cycles per second. The amplitude of the throttle area variation was maintained constant over the entire range of frequencies for each run and was kept small relative to the mean open area to avoid nonlinear effects. At each frequency,

the values of the in-phase and quadrature components of the several pressure perturbations were read on the transfer-function analyzer. The mean pressure drop across the downstream orifice was constant during each run, but was changed from run to run to vary the orifice impedance. The exit orifice impedance was determined for each run from the slope of the steady-state pressure-flow curve.

The following dimensionless pressure-perturbation ratios were computed from the data for each frequency:

(1) P_E/P_A

(2) P_F/P_A

(3) P_B/P_A

(Symbols are defined in appendix A.)

ANALYSIS

The system to be analyzed consists of a straight main pipe of length l and a branch of the same diameter and of length kl, which is attached to the main line at a distance xl from the downstream end, as shown in figure 2. The downstream end of the main line E (fig. 2) is terminated in an arbitrary load impedance Z_E. The end of the branch F is closed by a rigid cap. The positive direction of flow is chosen from A to E in the main line and from D to F in the branch. With this convention for the direction of the exit flow perturbation Q_E, the exit load impedance is defined by

$$Z_E = \frac{P_E}{Q_E} \tag{1}$$

This equation represents the impedance looking into the terminating structure from the end of the pipe.

In the following analysis, dimensionless complex numbers are used to represent pressure and flow perturbations and their ratios. The amplitude and phase of the various sinusoidal perturbations and their ratios are related to the corresponding complex numbers according to the usual conventions. Dimensionless pressure and flow perturbations and impedance are defined as follows:

$$p = \frac{P}{\rho c^2} \tag{2}$$

$$q = \frac{Q}{cS} \tag{3}$$

$$z = \frac{p}{q} = \frac{ZS}{\rho c} \tag{4}$$

A dimensionless frequency parameter defined by

$$\beta = \frac{2\pi f l}{c} \tag{5}$$

represents the phase shift in the distance l for a single sinusoidal wave train of frequency f and propagation speed c.

It is assumed that undamped sinusoidal acoustic waves exist in the system, that the pipe does not move longitudinally in response to the pressure perturbations, and that the mean fluid flow speed in the main line is negligible compared to the sonic speed. The acoustic line equations (derived in ref. 4) relating the pressure and flow perturbations at the two ends of a straight section of uniform pipe are, for section CE (fig. 2),

$$p_C = p_E \cosh ix\beta + q_E \sinh ix\beta \tag{6a}$$

$$q_C = q_E \cosh ix\beta + p_E \sinh ix\beta \tag{6b}$$

$$p_E = p_C \cosh ix\beta - q_C \sinh ix\beta \tag{6c}$$

$$q_E = q_C \cosh ix\beta - p_C \sinh ix\beta \tag{6d}$$

The following similar equations apply for sections AB and DF, the phase shifts being $(1 - x)\beta$ and $k\beta$, respectively:

$$p_A = p_B \cosh i(1 - x)\beta + q_B \sinh i(1 - x)\beta \tag{7a}$$

$$q_A = q_B \cosh i(1 - x)\beta + p_B \sinh i(1 - x)\beta \tag{7b}$$

$$p_B = p_A \cosh i(1 - x)\beta - q_A \sinh i(1 - x)\beta \tag{7c}$$

$$q_B = q_A \cosh i(1 - x)\beta - p_A \sinh i(1 - x)\beta \tag{7d}$$

$$p_D = p_F \cosh ik\beta + q_F \sinh ik\beta \tag{8a}$$

$$q_D = q_F \cosh ik\beta + p_F \sinh ik\beta \tag{8b}$$

$$p_F = p_D \cosh ik\beta - q_D \sinh ik\beta \tag{8c}$$

$$q_F = q_D \cosh ik\beta - p_D \sinh ik\beta \tag{8d}$$

The impedance relation at the downstream end (station E) is

$$\frac{p_E}{q_E} = z_E \tag{9}$$

The impedance at the closed end of the branch (station F) is infinite; hence,

$$\frac{q_F}{p_F} = \frac{1}{z_F} = 0 \tag{10}$$

Continuity of flow and pressure at the junction point is expressed by

$$q_B = q_C + q_D \tag{11}$$

and

$$p_B = p_C = p_D \tag{12}$$

The corresponding impedance relation is

$$\frac{1}{z_B} = \frac{1}{z_C} + \frac{1}{z_D} \tag{13}$$

where z_D is the impedance looking into the branch from the junction, z_C is looking downstream from the junction in the main line, and z_B is looking into the junction from the upstream side.

Transfer functions relating the various perturbations were obtained from equations (6) to (13) (mathematical details in appendix B). The relations among the perturbations at the two ends of the main line are conveniently expressed in terms of four functions of β, k, and x defined as follows:

$$\left.\begin{aligned} T &= \cos\beta - \tan k\beta \cos x\beta \sin(1 - x)\beta \\ U &= \sin\beta - \tan k\beta \sin x\beta \sin(1 - x)\beta \\ V &= \cos\beta - \tan k\beta \sin x\beta \cos(1 - x)\beta \\ W &= \sin\beta + \tan k\beta \cos x\beta \cos(1 - x)\beta \end{aligned}\right\} \tag{14}$$

In terms of these functions, the entrance impedance (looking downstream at point A) is

$$z_A = \frac{Tz_E + iU}{V + iz_E W} \tag{15}$$

The interterminal pressure ratio is

$$\frac{p_A}{p_E} = T + \frac{iU}{z_E} \tag{16}$$

The interterminal flow ratio is

$$\frac{q_A}{q_E} = V + iz_E W \tag{17}$$

Other ratios of possible interest are

$$\frac{p_A}{q_E} = Tz_E + iU \tag{18}$$

and

$$\frac{p_E}{q_A} = \frac{z_E}{V + iz_E W} \tag{19}$$

Equations (14) to (19) define the dynamic behavior of the system in terms of the pressure and flow perturbations at the terminals of the main line. In the experimental investigation, pressure perturbations were also measured at the junction point and at the closed end of the branch. Relations (derived in appendix B) involving p_B and p_F required for comparison with experimental results are as follows:

$$\frac{p_F}{p_A} = \frac{z_E \cos x\beta + i \sin x\beta}{\cos k\beta(Tz_E + iU)} \tag{20}$$

$$\frac{p_B}{p_A} = \frac{z_E \cos x\beta + i \sin x\beta}{Tz_E + iU} \tag{21}$$

RESULTS AND DISCUSSION

Pressure perturbations measured at stations B, C, and D on the three sides of the tee agreed within the limits of experimental error and, thus, verified the assumption of identical pressure perturbations in all branches at the junction point. Calculated and experimental pressure perturbation ratios are presented in figures 3 to 5. The curves were calculated from equations (16), (20), and (21); data points were determined from experimental measurements as described in the section Procedure. The ratio of downstream to upstream pressure is shown in figure 3. Figure 4 gives the ratio of pressure at the closed end to upstream pressure, and figure 5 gives the ratio of pressure at the junction point to upstream pressure. The experimental and analytical results are in agreement, which shows that classical undamped acoustic-wave theory provides a good description of the actual fluid wave motion for the conditions of the experiment (low-viscosity liquid and mean flow speed small compared to sonic speed).

The expressions for impedance and flow-perturbation ratios given in equations (15), (17), (18), and (19) could not be checked experimentally because flow perturbations were not measured, but the successful verification of equations (16), (20), and (21) is reason for confidence in the applicability of the others. Values of the upstream impedance calculated from equation (15) for the

experimental configuration ($k = x = 0.5$) are shown in figure 6.

Because of the complete reflection of waves at the closed end of the branch line, the system exhibits strong resonances at frequencies making the branch length an odd multiple of 1/4 wavelength ($k\beta = \pi/2, 3\pi/2$, etc.). At these frequencies the impedance looking into the branch is practically zero, and the pressure perturbation at the junction is, therefore, infinitesimal. Under these conditions, the branch accepts practically the entire flow perturbation entering the tee from the upstream line, and virtually no wave motion exists in the main line downstream of the junction.

CONCLUDING REMARKS

The results of this experiment and the two preceding investigations at this research center (refs. 3 and 4) indicate that undamped acoustic-wave theory derived for stationary fluids satisfactorily describes disturbance propagation in liquids flowing within long propellant lines, provided that any motion of the line itself is taken into account. Three different configurations, a straight line, a 90° L, and an equilateral T, were tested.

Similar analytical methods based on undamped wave theory would be expected to apply to small perturbations in other propellant-line configurations under the following conditions:

(1) Mean flow speeds up to about 20 feet per second

(2) Length-to-diameter ratios to about 1000

(3) Frequencies to about 100 cycles per second

(4) Fluids of low kinematic viscosity and high sonic speed such as water, kerosene, alcohol, liquid metals, and subcooled liquefied gases

Lewis Research Center
National Aeronautics and Space Administration
Cleveland, Ohio, May 10, 1963

APPENDIX A

SYMBOLS

c	sonic speed, ft/sec
f	frequency of sinusoidal perturbation, cps
k	ratio of branch to main-line length, dimensionless
l	length of main line, ft
P	perturbation pressure (complex number), lb/sq ft
p	dimensionless perturbation pressure (complex number), $P/\rho c^2$
Q	perturbation flow (complex number), cu ft/sec
q	dimensionless perturbation flow (complex number), Q/cS
S	inside area of cross section of pipe, sq ft
T,U,V,W	function of β, x, and k defined by eq. (14), dimensionless
x	position coordinate of junction (ratio of distance from exit to junction to main-line length), dimensionless
Z	acoustic impedance, $(lb)(sec)/ft^5$
z	dimensionless acoustic impedance (complex number), $ZS/\rho c$
β	frequency parameter, $2\pi fl/c$, dimensionless
ρ	mean fluid density, slugs/cu ft

Subscripts:

A,B,C,D,E,F	reference stations located as shown in fig. 2

APPENDIX B

DERIVATIONS

Transfer functions relating the various perturbations of interest may be obtained conveniently by determining the ratio of each to the exit pressure pertubation p_E.

From equations (6), (9), and (12)

$$\frac{p_C}{p_E} = \frac{p_B}{p_E} = \frac{p_D}{p_E} = \cosh i x\beta + \frac{\sinh i x\beta}{z_E} \tag{B1}$$

and

$$\frac{q_C}{p_E} = \frac{\cosh i x\beta}{z_E} + \sinh i x\beta \tag{B2}$$

From equations (8) and (10)

$$\frac{p_D}{p_F} = \cosh ik\beta \tag{B3}$$

and

$$\frac{q_D}{p_F} = \sinh ik\beta \tag{B4}$$

The ratios p_F/p_E and q_D/p_E are found as follows:

$$\frac{p_F}{p_E} = \frac{p_F}{p_D}\frac{p_D}{p_E} = \frac{\cosh i x\beta + \frac{\sinh i x\beta}{z_E}}{\cosh ik\beta} \tag{B5}$$

$$\frac{q_D}{p_E} = \frac{q_D}{p_F}\frac{p_F}{p_E} = \tanh ik\beta\left(\cosh i x\beta + \frac{\sinh i x\beta}{z_E}\right) \tag{B6}$$

From equation (11)

$$\frac{q_B}{p_E} = \frac{q_C}{p_E} + \frac{q_D}{p_E} \tag{B7}$$

Substituting from equations (B2) and (B6) gives

$$\frac{q_B}{p_E} = \sinh ix\beta + \tanh ik\beta \cosh ix\beta + \frac{1}{z_E}(\cosh ix\beta + \tanh ik\beta \sinh ix\beta)$$

(B8)

When equation (7a) is divided by p_E,

$$\frac{p_A}{p_E} = \frac{p_B}{p_E} \cosh i(1 - x)\beta + \frac{q_B}{p_E} \sinh i(1 - x)\beta \tag{B9}$$

Substituting from equations (B1) and (B8) and simplifying result in

$$\frac{p_A}{p_E} = \cosh i\beta + \tanh ik\beta \cosh ix\beta \sinh i(1 - x)\beta$$

$$+ \frac{1}{z_E}\left[\sinh i\beta + \tanh ik\beta \sinh ix\beta \sinh i(1 - x)\beta\right] \tag{B10}$$

Replacing hyperbolic with trigonometric functions and using the notation of equations (14) give

$$\frac{p_A}{p_E} = T + \frac{iU}{z_E} \tag{16}$$

When equation (7b) is divided by p_E,

$$\frac{q_A}{p_E} = \frac{q_B}{p_E} \cosh i(1 - x)\beta + \frac{p_B}{p_E} \sinh i(1 - x)\beta \tag{B11}$$

Substituting from equations (B1) and (B8), simplifying, and using the functions defined by equations (14) give

$$\frac{q_A}{p_E} = \frac{V}{z_E} + iW \tag{B12}$$

Equation (19) is the reciprocal of (B12).

$$\frac{p_E}{q_A} = \frac{z_E}{V + iz_E W} \tag{19}$$

The product of equations (16) and (19) is

$$z_A = \frac{Tz_E + iU}{V + iz_E W} \tag{15}$$

Multiplying equation (16) by equation (9) yields

$$\frac{p_A}{q_E} = Tz_E + iU \tag{18}$$

The product of equations (9) and (B12) is

$$\frac{q_A}{q_E} = V + iz_E W \tag{17}$$

Dividing equation (B5) by equation (16) and replacing hyperbolic by trigonometric functions give

$$\frac{p_F}{p_A} = \frac{z_E \cos x\beta + i \sin x\beta}{\cos k\beta(Tz_E + iU)} \tag{20}$$

The ratio p_B/p_A, obtained in the same way from equations (B1) and (16), is given by

$$\frac{p_B}{p_A} = \frac{z_E \cos x\beta + i \sin x\beta}{Tz_E + iU} \tag{21}$$

REFERENCES

1. Chang, S. S. L.: Transient Effects of Supply and Connecting Conduits in Hydraulic Control Systems. Franklin Inst. Jour., vol. 262, no. 6, Dec. 1956, pp. 437-452.

2. Sabersky, Rolf H.: Effect of Wave Propagation in Feed Lines on Low-Frequency Rocket Instability. Jet Prop., vol. 24, no. 3, May-June 1954, pp. 172-174.

3. Regetz, John D., Jr.: An Experimental Determination of the Dynamic Response of a Long Hydraulic Line. NASA TN D-576, 1960.

4. Blade, Robert J., Lewis, William, and Goodykoontz, Jack H.: Study of a Sinusoidally Perturbed Flow in a Line Including a 90° Elbow with Flexible Supports. NASA TN D-1216, 1962.

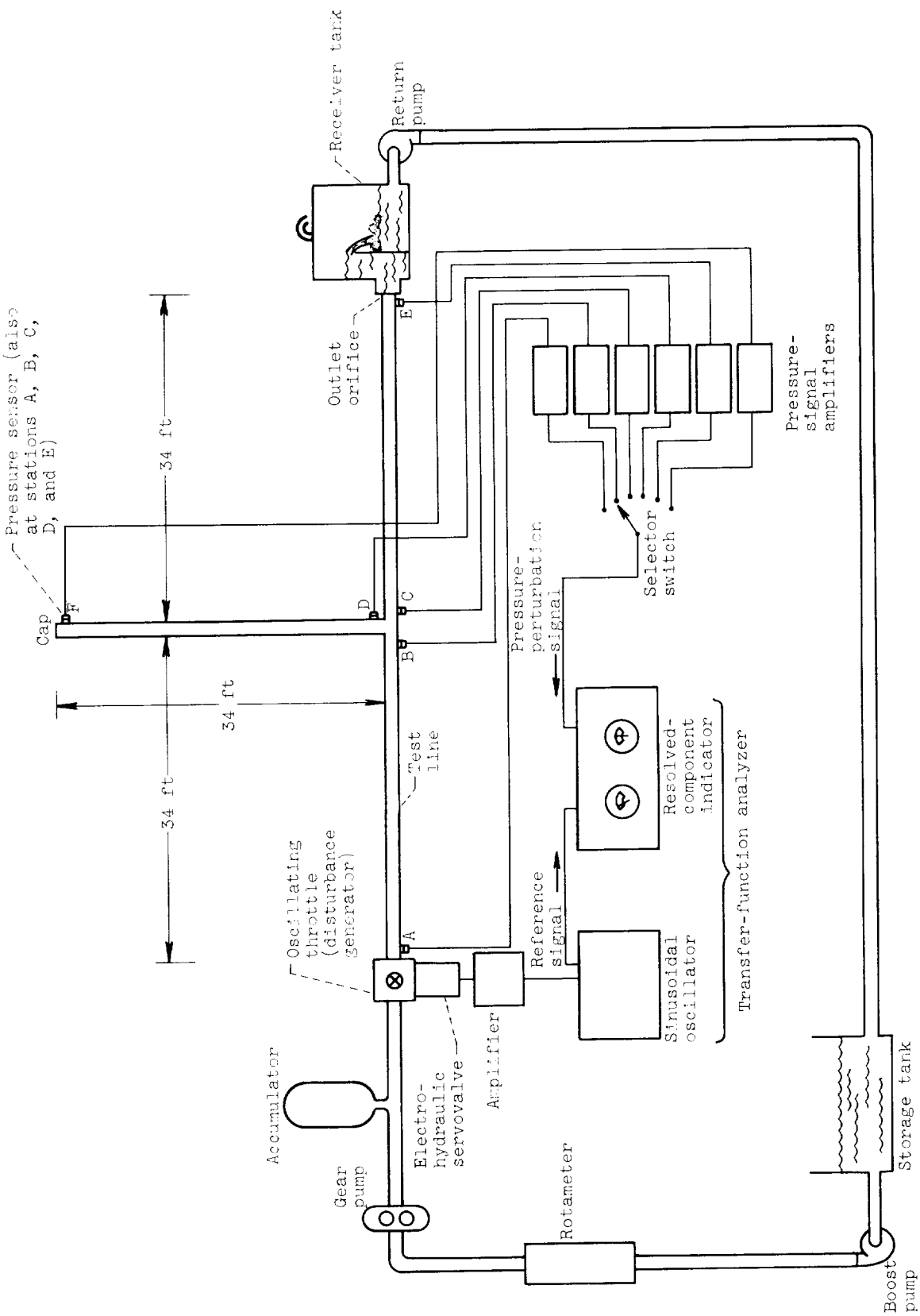

Figure 1. - Schematic diagram of hydraulic-line test apparatus.

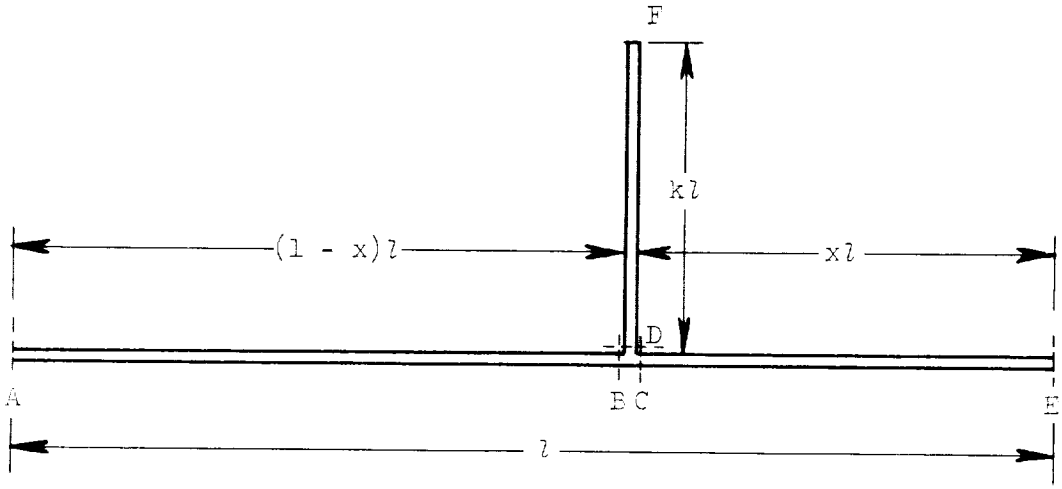

Figure 1. - General configuration of line with branch used in analysis.

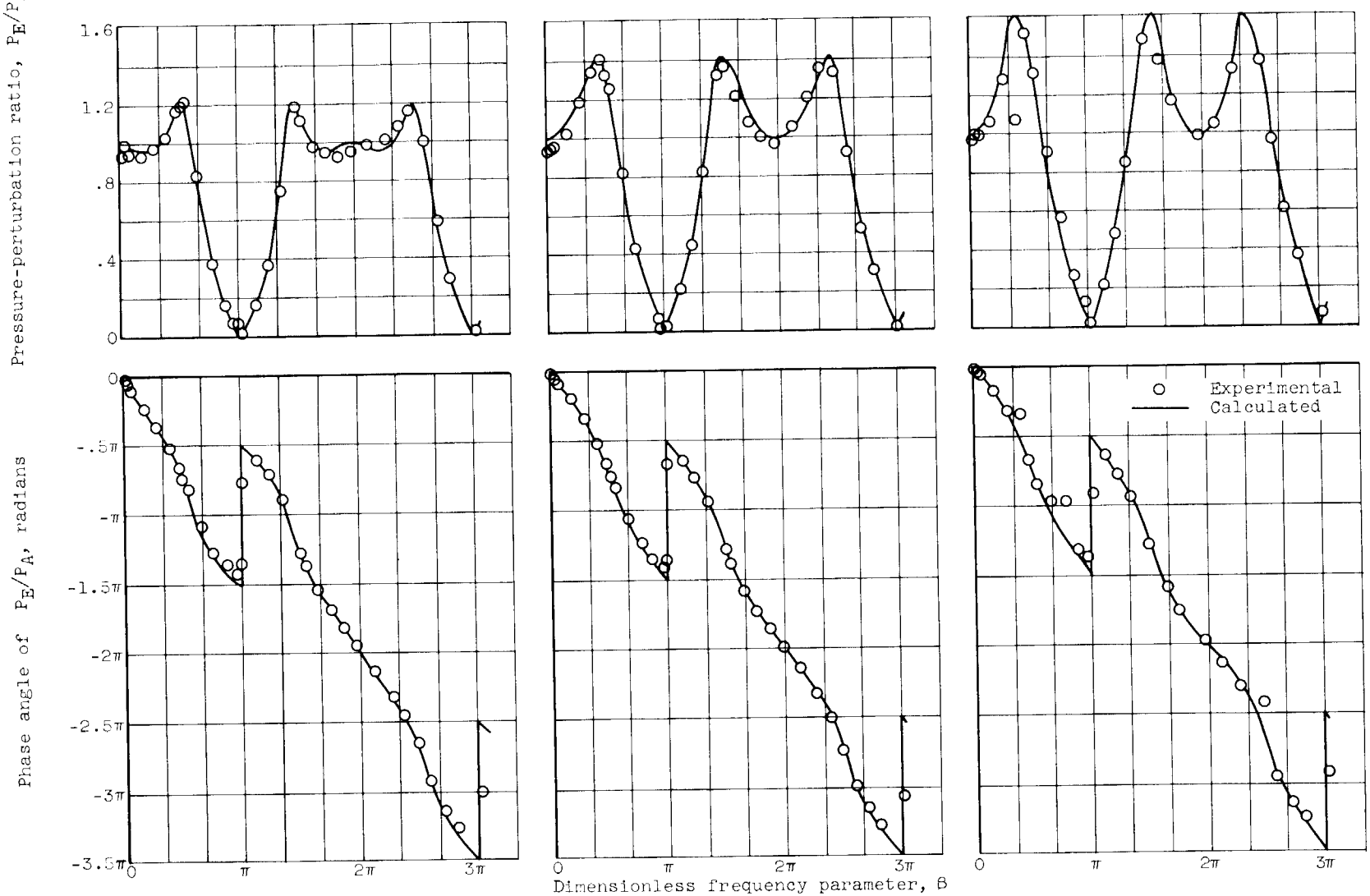

(a) Impedance at exit, z_E, 0.715. (b) Impedance at exit, z_E, 0.97. (c) Impedance at exit, z_E, 1.12.

Figure 3. - Ratio of pressure perturbation at exit to that at entrance.

(a) Impedance at exit, z_E, 0.715. (b) Impedance at exit, z_E, 0.97. (c) Impedance at exit, z_E, 1.12.

Figure 4. - Ratio of pressure perturbation at end of branch to that of entrance.

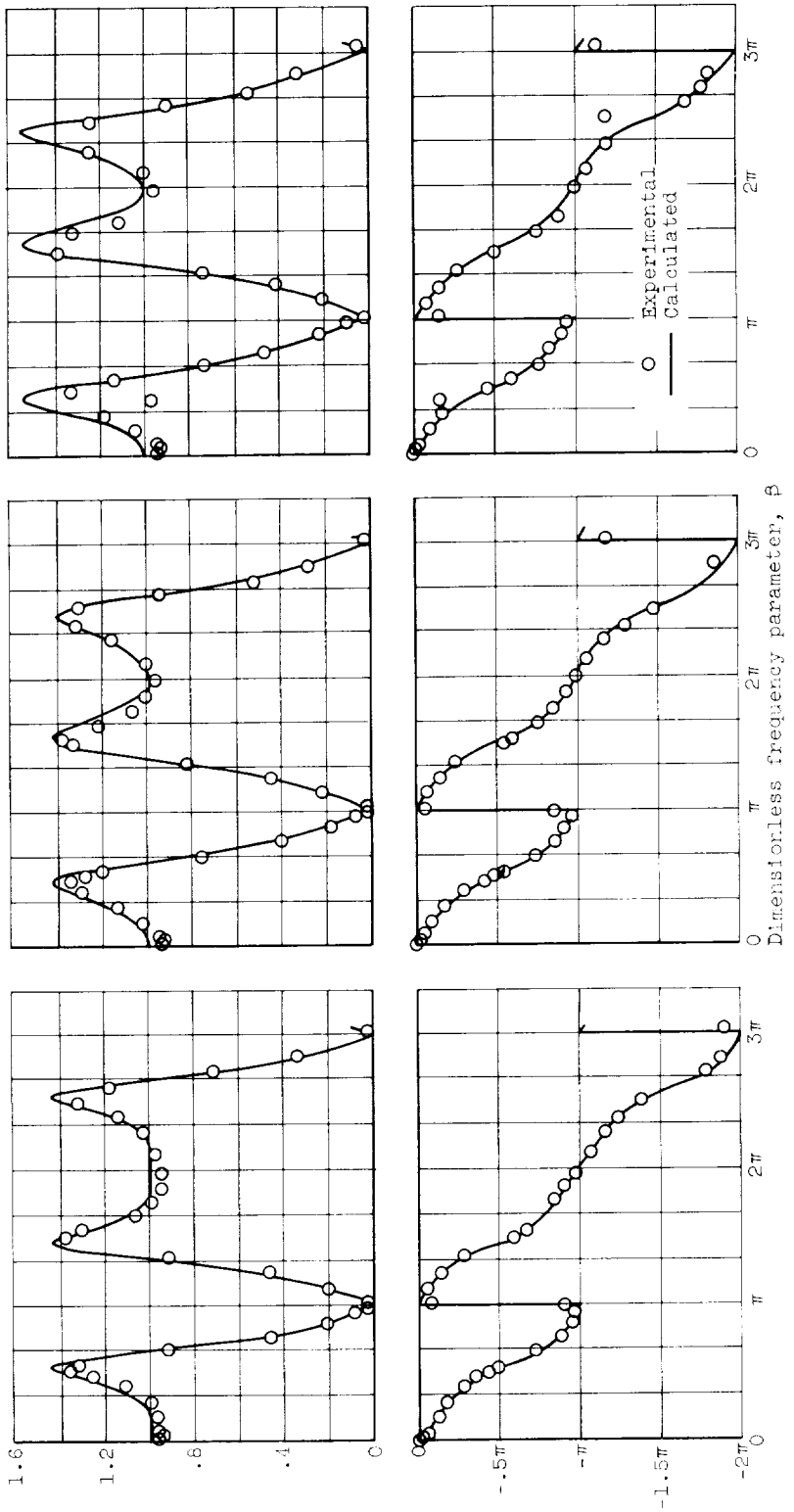

(a) Impedance at exit, z_E, 0.715. (b) Impedance at exit, z_E, 0.37 (c) Impedance at exit, z_E, 1.12.

Figure 5. - Ratio of pressure perturbation at junction to that at entrance.

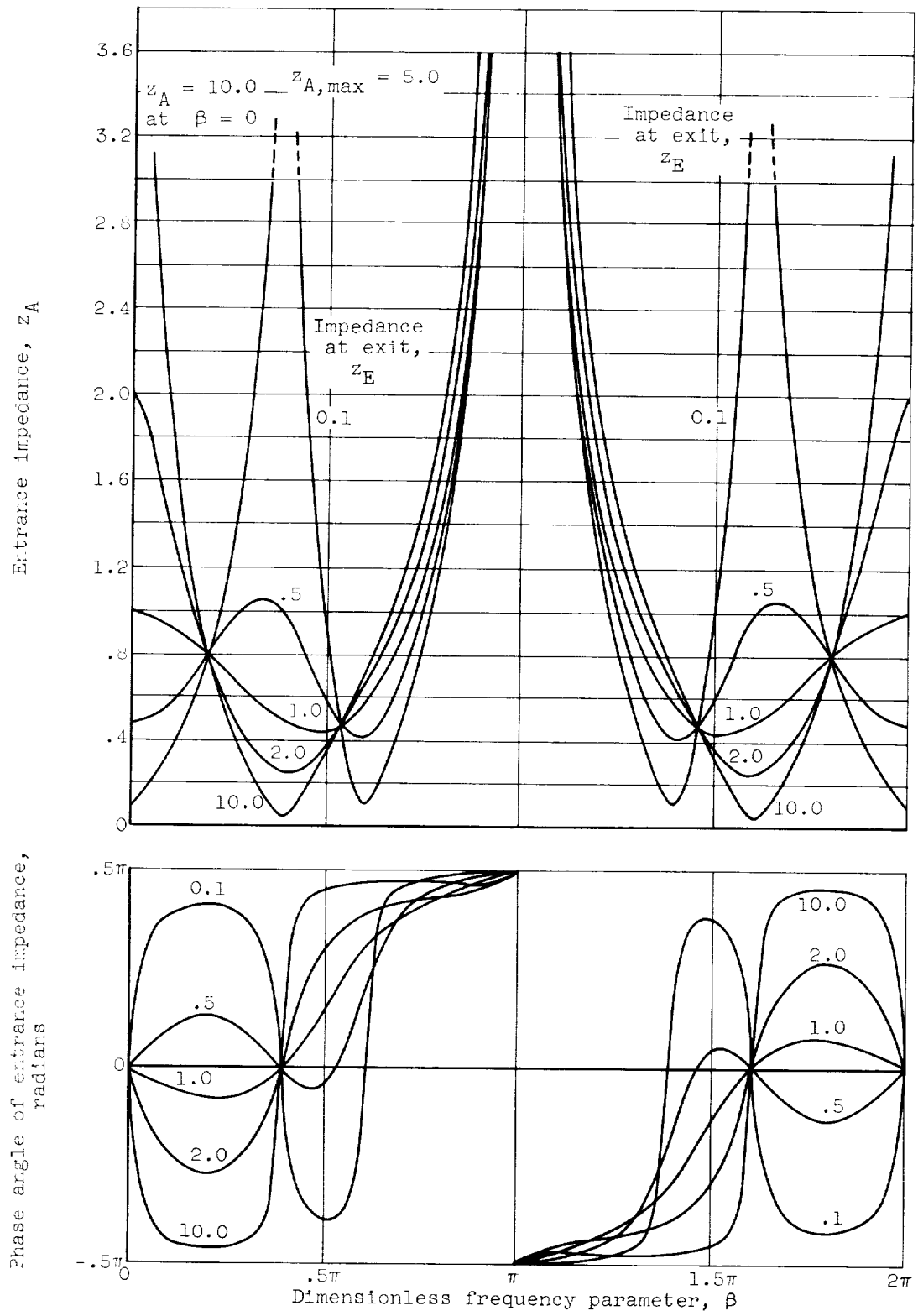

Figure 6. - Calculated entrance impedance z_A of equilateral branch line. (Values of z_A calculated by using equation (15) with $x = k = 0.5$.)

NASA-Langley, 1963 E-2036